where M_{B^*} and M_B refer to the masses of the members of the decuplet and the baryon octet respectively. $g_{B^*,BP}{}^0$ are determined by $SU(3)$ symmetry and they are given by

$$G=g_{N^*,N\pi}{}^0=-g_{N^*,\Sigma K}{}^0=-(\sqrt{6})g_{Y^*,\Sigma\pi}{}^0=-\sqrt{2}g_{Y^*,\Lambda\pi}{}^0=(\sqrt{6})g_{Y^*,N\bar{K}}{}^0=(\sqrt{6})g_{Y^*,\Xi K}{}^0$$
$$=\sqrt{2}g_{Y^*,\Sigma\eta}{}^0=(\sqrt{6})g_{\Xi^*,\Sigma\bar{K}}{}^0=-(\sqrt{6})g_{\Xi^*,\Xi\pi}{}^0=\sqrt{2}g_{\Xi^*,\Lambda\bar{K}}{}^0=-\sqrt{2}g_{\Xi^*,\Xi\eta}{}^0=g_{\Omega,\Xi\bar{K}}{}^0. \quad \text{(A10)}$$

$\bar{B}BP$ Interactions

With the usual decomposition of the interactions into isotopic spin representation and (5.11), we have

$$g_{BB'P}=g_{BB'P}{}^0\frac{1}{18}\left(\frac{(M_B+M_{B'})^2}{M_BM_{B'}}-\frac{m_P{}^2}{M_BM_{B'}}\right)\left(1+\frac{M_B+M_{B'}}{m_\rho}\right), \quad \text{(A11)}$$

where $g_{BB'P}{}^0$ are determined by exact $SU(3)$ symmetry and a D/F ratio of $\frac{3}{2}$. Thus

$$g_{NN\pi}{}^0=5(G/\sqrt{2}),\quad g_{\Lambda NK}{}^0=-3\sqrt{3}(G/\sqrt{2}),\quad g_{NN\eta}=\sqrt{3}(G/\sqrt{2}),$$
$$g_{\Lambda\Sigma\pi}{}^0=2\sqrt{3}(G/\sqrt{2}),\quad g_{\Sigma NK}{}^0=G/\sqrt{2},\quad g_{\Lambda\Lambda\eta}=-2\sqrt{3}(G/\sqrt{2}),$$
$$g_{\Sigma\Sigma\pi}{}^0=4(G/\sqrt{2}),\quad h_{\Lambda\Xi K}=\sqrt{3}(G/\sqrt{2}),\quad g_{\Sigma\Sigma\eta}=2\sqrt{3}(G/\sqrt{2}),$$
$$g_{\Xi\Xi\pi}{}^0=-G/\sqrt{2},\quad h_{\Sigma\Xi K}=-5(G/\sqrt{2}),\quad g_{\Xi\Xi\eta}=-3\sqrt{3}(G/\sqrt{2}).$$

The γ_μ- and $\sigma_{\mu\nu}$-type $\bar{\mathbf{B}}\mathbf{BV}$ interactions can be easily read from Table III.

PHYSICAL REVIEW VOLUME 139, NUMBER 5B 6 SEPTEMBER 1965

Summing Certain ϕ^4 Graphs Using Integral Equations*

S. Nussinov
University of Washington, Seattle, Washington
(Received 23 April 1965)

It is shown that the problem of summing certain graph chains occurring in ϕ^4 theory in which we have three (or four) particles in the intermediate state is reducible to an integral equation. For forward scattering and zero-mass field, this equation can be solved exactly using a method for solving the Bethe-Salpeter equation which has been recently suggested. As an example, the case of the truss-bridge diagrams is worked out in detail.

INTRODUCTION

An exact solution for the forward-scattering Bethe-Salpeter equation in ϕ^4 theory for zero internal masses and a kernel which is any arbitrary finite sum of irreducible primitively divergent graphs was recently obtained.[1] This was achieved by Wick-rotating and performing a four-dimensional partial-wave projection,[2] and finally utilizing the dilatational invariance by transforming to Mellin space[3] and obtaining by simple algebraic calculation an exact solution. It was shown that the inverse Mellin transform yields a partial-wave amplitude with fixed cuts.[4]

In the present paper we show that integral equations can be used to sum a certain class of diagrams—those shown schematically in Figs. 1 and 2. These diagrams do not contain two-particle intermediate states so that their formal sum does not lead to the ordinary Bethe-Salpeter equation. However, these diagrams may be divided into links by cutting across a line and a vertex or 2 vertices. This will allow us to write down simple

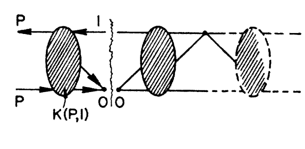

FIG. 1. Generalized diagrams which are separable by cutting across a line and a vertex.

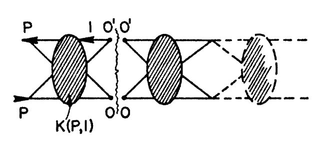

FIG. 2. Generalized diagram separable by cutting across two vertices.

* Supported in part by the U. S. Atomic Energy Commission under contract A.T. (45-1)-1388, program B.
[1] M. K. Banerjee, M. Kugler, C. A. Levinson, and I. J. Muzinich, Phys. Rev. **137**, B1280 (1965).
[2] J. D. Bjorken, J. Math. Phys. **5**, 192 (1964).
[3] P. Morse and H. Feshbach, *Methods of Theoretical Physics*, (McGraw-Hill Book Company, Inc., New York, 1953), Vol. 1, p. 976 ff.
[4] The fixedness of the cut is shown in detail in a forthcoming paper.

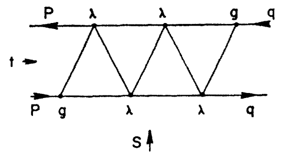

FIG. 3. An irreducible "truss-bridge" diagram.

integral equations for their sum which are amenable to the same treatment which was used in Ref. (1) in the case of the forward-scattering Bethe-Salpeter equation. The class of diagrams treated contains in particular the "irreducible truss bridge" diagrams (Fig. 3).[5] This case was first treated by Bjorken and Wu[6] and the fixed-cut behavior was demonstrated by finding an asymptotic behavior $A(s)\sim s^{n_0}(\ln s)^{-\frac{3}{2}}$. We will first treat this case in detail. This will serve as an illustration of the relative simplicity with which branch points are allocated using the present method.

(A) Let us denote the contribution of the irreducible truss bridge with μ "rungs" (Fig. 4) by $A^{\mu}(p,q)$. As suggested by Fig. 4, $A^{\mu}(p,q)$ may be related to $A^{\mu-1}(p,q)$ by performing all loop integrations except for the leftmost two:

$$A^{\mu}(p,q)=\frac{\lambda^2}{(2\pi)^8}\int\int\frac{d^4kd^4l A^{(\mu-1)}(l,q)}{(p-k)^2k^2l^2(l-k)^2}. \qquad (1)$$

In (1) we have assumed zero internal masses and adopted the notation of Refs. 1 and 7—the last one containing a comprehensive discussion of ϕ^4 renormalizability. Important for the derivation of (1) was the simplifying feature that the part of the diagram to the right of the broken line in Fig. 4 does not depend on each of the "external" momenta incident at the vertex 0, but only on their sum l. This part is practically the same as $A^{\mu-1}(l,q)$. This is true only up to a factor λ/g which results from the fact that 0 is a four-particle vertex, whereas in $A^{\mu-1}(p,q)$ it is a three-particle vertex. The cancellation of g in (1) reflects the fact that the introduction of the $g\phi^3$ interaction is just an artifice used in order to convert a two-particle intermediate state into a three-particle intermediate state and vice versa at the two ends of the ladder. Equation (1) suggests that $A=\sum_1^{\infty}A^{\mu}(p,q)$ is given by solving the integral equation

$$A(p,q)=B(p,q)+\frac{\lambda^2}{(2\pi)^8}\int\frac{d^4kd^4l}{(p-k)^2k^2l^2(l-k)^2}A(l,q), \qquad (2)$$

where $B(p,q)$ is the simplest bridge which cannot be further reduced, i.e., the one-meson exchange

$$B(p,q)=g^2/(p-q)^2. \qquad (3)$$

The k^0, l^0 integration contours can both be rotated to the respective imaginary axes (cf., Appendix A), and we can use 4-dimensional spherical harmonics expansion to simplify the resulting "Euclidean" integral equation. Expanding, we have

$$A=\sum A_n(p^2,q^2)C_n(\cos(\hat{p},\hat{q}))$$
$$(p-q)^{-2}=\sum(pq)^{-1}(p_</q_>)^{n+1}C_n(\cos(\hat{p},\hat{q})), \qquad (4)$$

where $C_n(\cos\theta)$ are the Tchebycheff polynomials,[1,2] and

$$p_</q_>=p/q \quad \text{for} \quad p<q$$
$$=q/p \quad \text{for} \quad q<p.$$

Writing similar expressions for $(p-k)^{-2}$, $(l-k)^{-2}$, substituting in Eq. (2), and using[8]

$$\int d\Omega_k d\Omega_l C_i(\cos(\hat{p},\hat{k}))C_j(\cos(\hat{k},\hat{l}))C_n(\cos(\hat{l},\hat{q}))$$
$$=(2\pi^2/(n+1))^2\delta_{ij}\delta_{jn}C_n(\cos(p,\hat{q})), \qquad (5)$$

the initial Eq. (2) separates into

$$A_n(p,q)=g^2B_n(p,q)+\frac{\lambda^2}{(n+1)^2(2\pi)^4 4}\times\int_0^{\infty}\int_0^{\infty}\frac{k^3dk}{k^2}\frac{l^3dl}{l^2}B_n(pk)B_n(kl)A_n(lq)$$

with

$$B_n(x,y)=(xy)^{-1}(x_</y_>)^{n+1}. \qquad (6)$$

The last equation can be rewritten as

$$A_n(p,q)=g^2B_n(p,q)+\frac{\lambda^2}{(n+1)^2(2\pi)^4 4}\times\int_0^{\infty}\int_0^{\infty}\frac{dk}{k}\frac{dl}{l}B_n'\left(\frac{l}{k}\right)B_n'\left(\frac{k}{p}\right)A_n(lq) \qquad (7)$$

with

$$B_n'(x,y)=(x/y)(x_</y_>)^{n+1}=B_n'(x/y). \qquad (8)$$

Equation (7) exhibits clearly the "dominance of $\lambda\phi^4$" in our mixed theory for the case of irreducible truss-bridge diagrams: The g^2 appears only in the inhomogeneous part and the kernel of Eq. (7) which is multi-

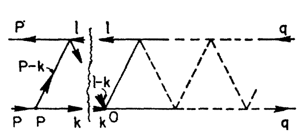

FIG. 4. The separation of a link for a truss bridge with μ "rungs."

[5] These diagrams contain a three-line vertices so that they arise only in a $\lambda\phi^4+g\phi^3$ theory. This, however, will not change crucially the results which, as will be seen, are typical of the dilatational invariant $\lambda\phi^4$ theory.

[6] J. D. Bjorken and T. T. Wu, Phys. Rev. 130, 2566 (1963).

[7] T. T. Wu, Phys. Rev. 125, 1436 (1962).

[8] This result is easily obtained by applying twice the relation $\int d\Omega_k C_i(\cos(\hat{p},k))C_j(\cos(\hat{k},\hat{l}))=[(2\pi)^2/(j+1)]\delta_{ij}C_j(\cos(\hat{p},\hat{l}))$ which is proved in Ref. 2.

plied by the dimensionless λ^2 only, exhibits the typical dilatational invariance of this theory. To utilize this invariance we take the Mellin transform of (7) with respect to p.[9] Applying twice the convolution theorem for Mellin transforms[10] we get

$$\bar{A}_n(\alpha,q)=g^2\bar{B}_n(\alpha,q) +\lambda^2[(n+1)^2(2\pi^4)]^{-1}\bar{B}_n'^2(\alpha)\bar{A}_n(\alpha,q)\,, \quad (9)$$

where from the definition of the Mellin transform and Eqs. (4) and (8) we have

$$\bar{B}_n(\alpha)=\tfrac{1}{2}[((n+2)+\alpha)^{-1}-(\alpha-n)^{-1}] =(n+1)/[(n+2)+\alpha](n-\alpha)$$
$$B_n(\alpha,q)=2q^{\alpha-2}B_n'(\alpha)\,. \quad (10)$$

We note that $\bar{B}_n'(\alpha)$ is meromorphic. $\bar{B}_n(\alpha,q)$ diverges in the limit $q\rightarrow 0$ unless $\mathrm{Re}\alpha>2$. This reflects the infrared divergence of the ϕ^3 part of the interaction which determines the inhomogeneous term in Eq. (9) when we put internal masses equal to zero. A nonzero internal mass will remedy this difficulty and as can be directly shown[11] will not affect the essential results about location of the cuts.

The integrand in the inverse Mellin transform relation

$$A_n(p,q)=\frac{1}{2\pi i}\int_{-i\infty}^{+i\infty}d\alpha\, p^{-\alpha}\bar{A}_n(\alpha,q) =\frac{1}{2\pi i}\int_{-i\infty}^{+i\infty}d\alpha\frac{p^{-\alpha}\bar{B}_n(\alpha,q)}{1-\rho\bar{B}_n'^2(\alpha)}\,, \quad (11)$$

{where ρ denotes $\lambda^2[(n+1)^2(2\pi)^4]^{-1}$} has four poles at the α_i satisfying

$$\left[\frac{\lambda}{(n+1)(2\pi)^2}\frac{(n+1)}{(n+2+\alpha_i)(n-\alpha_i)}\right]^2=1\,,$$
$$\frac{1}{(n+2+\alpha_i)(n-\alpha_i)}=\pm\frac{(2\pi)^2}{\lambda}\,, \quad (12)$$

so that

$$\alpha_i(n)=-1+(1\mp\lambda/(2\pi)^2+n^2+2n)^{1/2}. \quad (12')$$

[The $\mp$ inside the square root correspond to the $\pm$ in Eq. (12).] Denoting the four α's given in Eq. (12′) by $\alpha(--)$, $\alpha(-+)$, $\alpha(+-)$, and $\alpha(++)$, we have for the residua contributed by the four poles the expressions

$$\mp\tfrac{1}{2}(n+1)(1\mp\lambda/(2\pi)^2+n^2+2n)^{-\frac{1}{2}}g^2q^{-2}(q/p)^{-\alpha_i(n)} =R_i((n)(p,q))\,. \quad (13)$$

Since the integration contour in Eq. (11) may be closed by an infinite semicircle in the right half α plane when $q<p$ and in the left half if $p<q$, we have

$$A_n(p,q)=\sum G_iR_i(n,(p,q)) \quad \text{for} \quad q<p$$
$$=\sum(1-G_i)R_i(n,(p,q)) \quad \text{for} \quad p<q \quad (14)$$

and

$$G_i=1 \quad \text{if} \quad \mathrm{Re}(\alpha_i)>0$$
$$=0 \quad \text{if} \quad \mathrm{Re}(\alpha_i)<0.$$

For the purpose of extracting the most important piece of information, the location of the square-root branch points in n, the exact solution (13) and (14) is unnecessary. These branch points result from branches in the $\alpha_i(n)$, the location of which can be read directly from Eq. (12′) to be

$$n_i=-1\pm[\pm\lambda/(2\pi)^2]^{1/2}; \quad (15)$$

for $\lambda>0$ the leading singularity is at

$$n_1=-1+[\lambda/(2\pi)^2]^{1/2}.$$

This result is identical with that of Ref. 6, if the different conventions used there are properly accounted for.[12]

Let us conclude this section with the remark that if we use $A_n(p,q)$ given by (13) and (14) as a kernel for an ordinary Bethe-Salpeter equation[13]

$$A_n'(p,q)=A_n(p,q)+\frac{1}{8\pi^2(n+1)}\int_0^\infty\frac{dk}{k}A_n(pk)A_n'(kq)\,, \quad (16)$$

then the solution of that equation will give the sum of all truss-bridge diagrams including the reducible truss bridges such as those shown in Fig. (5). If appropriate care is taken of the apparent low-limit divergence of Eq. (16) [cf. remark following Eq. (10)], this is even a Fredholm-type equation due to the q^{-2} factor in $A_n(pk)$ [see Eq. (13)] which makes the kernel of Eq. (16) die off sufficiently rapidly at infinity so that it is square-integrable. Thus the solution $A_n'(p,q)$ viewed as a

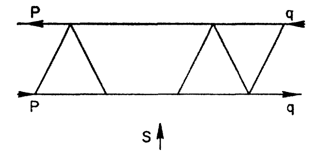

FIG. 5. A reducible truss bridge.

[9] The Mellin transform $\bar{f}(\alpha)$ of $f(x)$ is defined by

$$\bar{f}(\alpha)=\int_0^\infty x^{\alpha-1}f(x)dx.$$

[10] The theorem states that the Mellin transform of $\int(dy/y)\times f(x/y)g(y)$ is $\bar{f}(\alpha)\bar{g}(\alpha)$; see, for example, Ref. 3.

[11] This will be shown in a forthcoming paper.

[12] This result coincides with that of Ref. 6 if attention is paid to the fact that the Lagrangian used there eliminates the $1/(2\pi)^4$ used in the present paper with each loop integration. I am indebted to Professor M. Baker for pointing this out.

[13] Writing (16) directly in Euclidean partial-wave representation entails the implicit assumption that the original Bethe-Salpeter equation with the sum of all irreducible "truss bridges" as a kernel can be rotated to Euclidean metric. For forward scattering this depends only on the kernel, but we proved this already in showing that Wick rotation is allowed in the integral equation for the irreducible truss bridges themselves (cf. Appendix A), so that the kernel $A(p,q)$ is defined only in terms of the continuation of the Euclidean $A(p,q)$. [A general recipe of continuation of any planar convergent graph from the Euclidean to the physical region is given by G. Tiktopoulos, Phys. Rev. **136**, B275 (1964).]

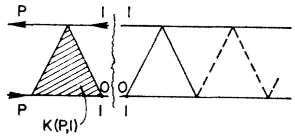

FIG. 6. Cutting an irreducible truss bridge across a line and a vertex.

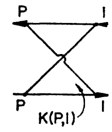

FIG. 8. The "unit" of the "nested-bridge" diagram.

function of n will "inherit" the fixed branch points of $A_n(p,q)$ and perhaps will also have some poles from the Fredholm determinant solution. If we would formulate the problem for non-forward-scattering,[4] this Regge pole $\alpha_0(t)$ would clearly move with t whereas the n_i are fixed. At a certain critical $t_c=t_c(g,\lambda)$, it may happen that $\mathrm{Re}\alpha_0(t)$ becomes greater than n_1. If one investigates only the asymptotic behavior, one will notice that at a critical t_c a "transition" in the asymptotic behavior from an $s^{+n_1}f(\ln s)$ to $s^{\alpha(t)}$ behavior [$f(\ln s)$ is some logarithmic function, $(\ln s)^{-3/2}$ for the present case according to Ref. 6]. Such a transition was indeed found in Ref. 6.

(**B**) Let us note now that after obtaining (2) we could derive from it a "one-vector" equation by performing the d^4k integration first:

$$A(p,q)=B(p,q)+\frac{\lambda^2}{(2\pi)^8}\int\frac{d^4l}{l^2}K(p,l)A(l,q)\,,$$
$$K(p,l)=\int\frac{d^4k}{(p-k)^2k^2(l-k)^2}\,. \tag{17}$$

Since on grounds of dimensionality $K(p,l)=K'(p,l)/l^2$, where $K'(p,l)$ is of zero power in momentum, (17) would yield upon four-dimensional partial-wave projection an equation of the type

$$A_n(p,q)=B_n(p,q)+\rho\int\frac{dl}{l}K_n'\left(\frac{p}{l}\right)A_n(l,q)\,; \tag{18}$$

so that applying directly the methods of Ref. 1, we would be able to conclude that *independent* of the particular form of $K_n'(x)$, Eq. (18) will yield an amplitude with fixed cuts in n. The actual evaluation of the branch point location in this way may be quite complicated and in the particular case of the irreducible truss bridges, the special method used above led easily to the results. Pictorially speaking, Eq. (17) would have been obtained directly if instead of cutting the diagram across three lines (l, $l-k$, k), as in Fig. 4, we would separate a whole triangular unit by cutting across one line (l) and a vertex 0 as shown in Fig. 6. The important point which applies also for the general diagram of the type shown in Fig. 1 is that both units on the left and right of the dividing line in Figs. 1 or 6 depend, after internal loop integration, only on the sum of the two

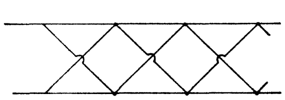

FIG. 7. A "nested-bridge" diagram as a particular example of graphs shown in Fig. 2.

vectors emanating from 0 so that a one-vector equation may be also written for the general case. In the case of forward scattering, this equation yields, upon four-dimensional partial wave projection, a relation which, owing to dilatational invariance, must have the form (18). Obtaining (18) and solving for the location of branch points by the method illustrated above may serve as a general recipe for the general diagram of the type Fig. 1. A further natural extension at this point is to consider chain graphs such that we can separate the iterated "units" by cutting across two vertices as those shown in Fig. 2. $K(p,l)$ could be the most general four-particle scattering graph. The same arguments as above lead to the conclusion that we can always reduce the problem to an integral equation like (18). One of the simplest conceivable diagrams of this type[14] is the "meshed bridges" diagram (Fig. 7). The "unit" $K(p,l)$ is the crossed box diagram shown in Fig. 8 and an exact four-dimensional partial wave analysis of it seems to be impractical.

Let us finally note that integral equations may be used to sum infinite series of diagrams generated in a simple recursive way other than the "generalized ladders" for which the usual Bethe-Salpeter equation or the above discussed methods are applicable. A simple interesting example is the "nested bubble" series shown in Fig. 9. The recursive relation between elements of this series yields (for the sum) the integral equation suggested by Fig. 10:

$$B(p^2)=B^0(p^2)+\frac{\lambda^2}{(2\pi)^8}\times\int\frac{d^4kd^4q\,B(q^2)}{k^2(p-k)^2(k-q)^2[p-(k-q)]^2}\,. \tag{19}$$

$B^0(p^2)$ denotes here the "bare bubble" diagram in which one subtraction has to be made. Equation (19) may be rewritten as

$$B(p^2)=B^0(p^2)+\lambda^2\int_0^\infty\frac{dq}{q}K'\left(\frac{p}{q}\right)B(p^2)\,, \tag{20}$$

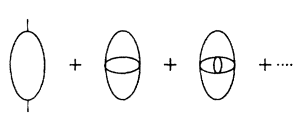

FIG. 9. The "nested-bubbles" series.

[14] Even a simpler case is the ordinary bubble-ladder diagrams which may alternatively be viewed as a sequence of squares connected at their vertices. However the analysis of this case by the ordinary Bethe-Salpeter equation considering it as bubbles connected by lines is well known and much simpler [Cf. M. Baker and I. J. Muzinich, Phys. Rev. **132**, 2291 (1963)].

where

$$K'(p/q)=q^4\langle K(p,q)\rangle \tag{20'}$$

and

$$K(p,q)=\frac{1}{(2\pi)^8}\int\frac{d^4k}{k^2(p-k)^2(k-q)^2[p-(k-q)]^2} \tag{20''}$$

which is the box diagram for forward scattering. In the above, we assumed that (19) can be transformed to an

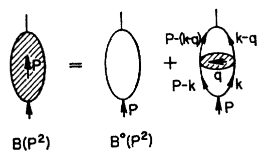

FIG. 10. A graphical representation of the integral equation for the "nested-bubbles" series.

Euclidean metric and we took the angular average (indicated by $\langle\ \ \rangle$) of $K(p,q)$ because it multiplies a function of p^2 only. The fact that K' is a function of (p/q) only follows from dimensional considerations. The Mellin transform method is immediately applicable to Eq. (20). Because of the $p\leftrightarrow q$ symmetry of $K'(p,q)$, $K(x)=K(1/x)$ and $\bar{K}(\alpha)=\bar{K}(-\alpha)^1$ so that poles of the Mellin transform $\bar{B}(\alpha)$ are symmetric with respect to the imaginary α axis, and a cut of $B_\lambda(p^2)$ will occur in $\lambda=\lambda_0$ which satisfies $1=\lambda_0\bar{K}(0)$ because then two poles of $\bar{B}_\lambda(\alpha)$ will coalesce and pinch the integration contour of the inverse Mellin transformation (11). This result suggests that beyond a certain λ_0 the "potential" itself will become complex. We note, in particular, that the self-regularizing mechanism suggested for the bubble diagram[15] will not be applicable in this case. If we use for the Bethe-Salpeter kernel the sum of all iterated bubbles (Fig. 11), the cut in λ will persist in the new kernel $B_\lambda'(s)$,

$$B_\lambda'(s)=\lambda^2B_\lambda(s)/[1-B_\lambda(s)], \tag{21}$$

and also in the solution of the Bethe-Salpeter equation. All the above suggests that the existence of branch points in the angular momentum and in the coupling constant are characteristic of the dilatational invariance

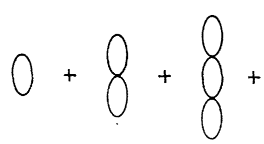

FIG. 11. "s channel" iteration of bubbles.

of $\lambda\phi^4$ theory and not of the particular approximations in the solution.

ACKNOWLEDGMENTS

It is a pleasure to thank Professor I. J. Muzinich for his help and encouragement. A helpful discussion with Professor M. Baker is gratefully acknowledged.

[15] P. Suranyi and J. Kiviecinsky, Phys. Letters **9**, 283 (1964).

APPENDIX A

Writing Eq. (4) in detail, we have

$$A(\mathbf{p}p^0,\mathbf{q}q^0)=B(\mathbf{p}p^0,\mathbf{q}q^0)+\frac{\lambda^2}{(2\pi)^8}\int\int d^3kd^3l \times\int dk^0dl^0AD^{-1}, \tag{A1}$$

$$D=[(\mathbf{p}-\mathbf{k})^2-(p^0-k^0)^2-i\epsilon][\mathbf{k}^2-k^{02}-i\epsilon] \times[\mathbf{l}^2-l^{02}-i\epsilon] \times[(\mathbf{l}-\mathbf{k})^2-(l^0-k^0)^2-i\epsilon]. \tag{A2}$$

We see that poles resulting from the vanishing of the various arguments in the denominator occur at

$$l^0=\{\pm|\mathbf{l}|\mp i\epsilon,\ k^0\pm|\mathbf{l}-\mathbf{k}|\mp i\epsilon\}\quad\text{for}\quad \mathbf{k},\mathbf{l},k^0\ \text{fixed}$$

and at

$$k^0=\{\pm|\mathbf{k}|\mp i\epsilon,\ l^0\pm|\mathbf{l}-\mathbf{k}|\mp i\epsilon,\ p^0\pm|\mathbf{p}-\mathbf{k}|\mp i\epsilon\}\quad\text{for}\quad \mathbf{k},\mathbf{l},l^0\ \text{fixed}. \tag{A3}$$

Let us perform Wick rotations[16] of both the k^0 and l^0

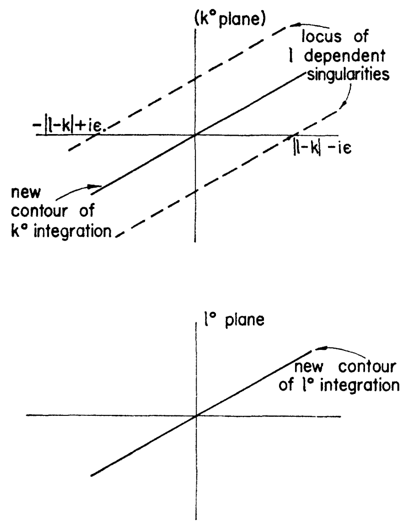

FIG. 12. Simultaneous k^0l^0 contour rotation.

contours at the same time:

$$k^0\longrightarrow e^{i\theta}k^0\quad l^0\longrightarrow e^{i\theta'}l^0,$$

where θ (θ') varies from 0 to $\frac{1}{2}\pi$. If we rotate both contours at the same rate, i.e., keeping them parallel to each other $\theta=\theta'$, we see that the l^0 integration contour will stay all the time parallel to the locus of k^0-dependent singularities [cf. (A3) and Fig. 12] and no k^0-dependent singularities are crossed throughout the process. The same applies when $k^0\leftrightarrow l^0$. As far as fixed singularities are concerned, the ordinary Wick procedure applies. We note that already in the original work[16] Wick mentions the possibility of simultaneous rotation of contours when using more complex kernels than those of the ladder type.

[16] G. C. Wick, Phys. Rev. **96**, 1124 (1954).